NEURODEVELOPMENT

A neurodevelopmental origin of behavioral individuality in the *Drosophila* visual system

Gerit Arne Linneweber[1,2,3], Maheva Andriatsilavo[1,2,3], Suchetana Bias Dutta[1,2,3], Mercedes Bengochea[1], Liz Hellbruegge[2,3], Guangda Liu[4,5], Radoslaw K. Ejsmont[1]*, Andrew D. Straw[6], Mathias Wernet[2], Peter Robin Hiesinger[2,3], Bassem A. Hassan[1,2,3]†

The genome versus experience dichotomy has dominated understanding of behavioral individuality. By contrast, the role of nonheritable noise during brain development in behavioral variation is understudied. Using *Drosophila melanogaster*, we demonstrate a link between stochastic variation in brain wiring and behavioral individuality. A visual system circuit called the dorsal cluster neurons (DCN) shows nonheritable, interindividual variation in right/left wiring asymmetry and controls object orientation in freely walking flies. We show that DCN wiring asymmetry instructs an individual's object responses: The greater the asymmetry, the better the individual orients toward a visual object. Silencing DCNs abolishes correlations between anatomy and behavior, whereas inducing DCN asymmetry suffices to improve object responses.

Individual variability in morphology is abundant, including among human identical twins and species that reproduce by parthenogenesis (*1*, *2*). In this regard, the brain is no exception. Examples of individual brain variation include differences of size, weight (*3*), and neuroanatomical parcellations of human brains (*4*, *5*). In invertebrates, where individual neurons can be identified across animals, single neurons show variability in morphology, wiring (*6*), synaptic connectivity, and molecular composition across individuals (*7*–*9*).

Similarly, innate behaviors, such as selective attention to stimuli, show individual variation even among genetically identical individuals (*10*–*13*). The stability of individual differences over time defines behavioral idiosyncrasies as animal individuality (*14*). It has been proposed that variability in innate behavior is due to neuromodulation of anatomically hardwired circuits (*15*–*17*). By contrast, there is evidence for developmental plasticity resulting in a range of possible circuit diagrams among individuals (*18*, *19*), but whether nonheritable individual anatomical differences in brain wiring can predict distinct behavioral outcomes is unexplored (*20*–*23*).

To test whether stochastic wiring of neural circuits affects behavioral variation, we used *Drosophila* contralateral visual interneurons called the dorsal cluster neurons (DCNs) (*24*) (also known as LC14) (*25*). DCNs exhibit up to 30% wiring variability of their axonal projections between individuals and between the left and right hemispheres of the same brain (*26*). DCN axons innervate two alternative target areas in the fly visual system called the medulla (M-DCNs) and the lobula (L-DCNs) (*24*). The decision whether any given DCN becomes a M-DCN or L-DCN is determined by an intrinsically stochastic lateral inhibition mechanism mediated by the Notch signaling pathway (*18*). To test the link between wiring variation and behavioral variation, we used a visual behavioral assay called Buridan's paradigm (*27*). In this assay, a fly is placed between two identical high-contrast stripes at 180° from each other in a uniformly illuminated arena (*28*). The stripes are unreachable, inducing the fly to walk back and forth between them during the assay.

Here we report that flies show behavioral individuality that is nonheritable and is not reduced through inbreeding. We find that the degree in left-right DCN wiring asymmetry in the medulla is a predictor of behavioral performance of individual flies. The more asymmetric the DCN medulla innervation is, the narrower the path a fly walks between the two stripes. DCN activity is necessary for this correlation, and reengineering DCN asymmetry suffices to change an individual's behavior.

Results

While analyzing object orientation responses in wild-type *Canton S* (*CS*) flies (Fig. 1A and movies S1 to S3), we noted sex-independent interindividual variability in their trajectories (Fig. 1, B and C). We focused on a parameter called absolute stripe deviation (henceforth aSD), measuring the deviation from the narrowest possible path between the stripes. Although males tend to walk narrower paths, the degree of interindividual variation in aSD is the same between males and females (Fig. 1D). We therefore continued our studies with combined populations (Fig. 1E).

Object orientation variability is independent of genetic diversity

To test whether behavioral variability correlates with genetic diversity, we screened a subset (N = 10) of the *Drosophila* genomic reference panel (DGRP) (*29*) for genetically homogeneous strains with extreme object orientation responses. This identified two strains with opposing behavioral phenotypes: *DGRP-639* showed low aSD (Fig. 1, F and G), whereas *DGRP-859* showed high aSD (Fig. 1, H and I). Similar behavioral differences were found in seven other representative behavioral parameters (fig. S1). However, despite the extreme reduction of genetic diversity, the degree of individual variation in aSD was not reduced (Fig. 1, G and I). On the contrary, *DGRP-639* showed increased behavioral variability (Fig. 1G and fig. S1), hinting at the nonheritability of this variability.

Individual object orientation responses are nonheritable

If the genotype of an individual determines its behavior, repeated breeding of parental animals with a specific behavioral trait should select for a specific behavior, creating a behaviorally homogeneous population. We mated three pairs with the lowest and highest aSD scores, respectively (Fig. 2, A and B), and object orientation responses were measured in their offspring (Fig. 2, C and D). We found no differences between the two sets of offspring in aSD scores as well as six other parameters tested (fig. S2A). The same was true for the offspring of a single pair with low and high aSD (fig. S2, B and C). We repeated the same breeding schemes with the near-isogenic *DGRP-639* and *DGRP-859* for seven generations. We found that for most parameters, a breeding pair reproduces the full range of variability in the population at every generation (figs. S3 and S4).

Individual object orientation responses are stable over time

An individual's idiosyncratic behavioral profile may not be heritable either because it is driven by internal-state modulations, or because it is driven by nonheritable developmental mechanisms. To distinguish these possibilities, we first tested the same individual *CS* flies once every other day for 3 days and found that an individual's behavior was virtually identical over the three trials (Fig. 3, A and B). Statistical analysis of aSD showed that the individual responses of *CS* flies on different days were correlated (r = 0.74 to 0.77, Fig. 3E). The same was true for

[1]Institut du Cerveau et de la Moelle Epinière (ICM)–Sorbonne Université, Inserm, CNRS, Hôpital Pitié-Salpêtrière, Paris, France. [2]Division of Neurobiology of the Institute for Biology, Free University, Berlin, Germany. [3]Einstein-BIH, Charité Universitätsmedizin, Berlin, Germany. [4]VIB Center for the Biology of Disease, VIB, 3000 Leuven, Belgium. [5]Center for Human Genetics, University of Leuven School of Medicine, 3000 Leuven, Belgium. [6]Institute of Biology I and Bernstein Center Freiburg, Faculty of Biology, Albert-Ludwigs-University Freiburg, Freiburg, Germany.
*Present address: Centre de Recherches Interdisciplinaires (CRI), 10 rue Charles V, 75004 Paris, France.
†Corresponding author. Email: bassem.hassan@icm-institute.org

path details like left- or right shifted angles (Fig. 3A and fig. S5C), distance, full walks, meander, absolute horizon deviation, absolute angle deviation, angle deviation, and center deviation. We extended this analysis over a 4-week period. We found that the object responses of individuals were stable over this extended period (Fig. 3, C and D, and fig. S6, A and B). This stability argued against state modulations and in favor of individual properties. Indeed, starvation followed by refeeding over a period of 3 days failed to reduce stability of individual performances despite obvious changes in mean population behavior (fig. S7). Finally, we asked whether

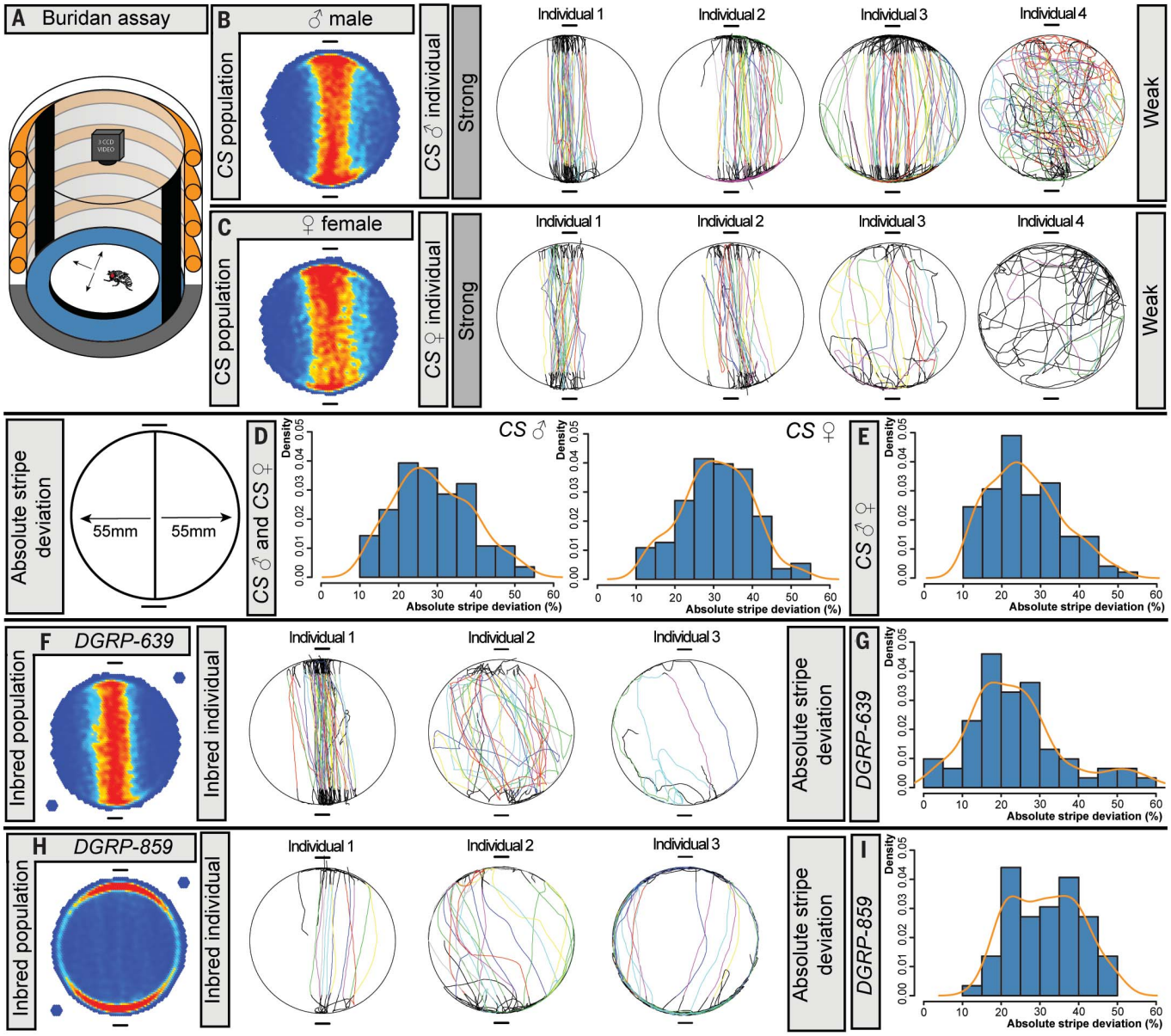

Fig. 1. Individual variation of *Drosophila* stripe responses is independent of gender or genetic diversity. (**A**) *Drosophila* object orientation responses are measured in a Buridan's paradigm arena. (**B**) Male *CS* wildtype flies (N = 50) showed on the population level (shown in a heatmap) an object orientation response toward the stripes that are located at the top and bottom. The categorization of individual responses into strong and weak object orientation responses shows the entire repertoire of responses (shown as individual fly tracks). (**C**) Female *CS* wild-type flies (N = 48) showed the same object orientation responses as their male counterparts. (**D**) The histograms for aSD show that *CS* male (N = 50) and female (N = 48) flies displayed the same range of individual responses. The histogram shows in bins of 5 % of the radius the distribution of aSD for each population. The distributions for males and females are statistically identical (Tukey test, p = 0.1). (**E**) The histogram shows the cumulative aSD for *CS* male and female flies (N = 98). (**F**) *DGRP-639* flies (N = 61) showed on the population level an object orientation response toward the stripes that exceeds even the response of *CS* (Tukey test, p = 0.01). Three examples of individual responses show the individual differences. (**G**) The histogram for aSD shows that *DGRP-639* flies (N = 61) exceed the variability of *CS* flies (F-test, $p < 0.001$). The distribution is shifted toward lower aSDs. (**H**) *DGRP-859* flies (N = 59) showed on the population level (heatmap) a weak object orientation response toward the stripes. The main population response is edge behavior. Two examples of individual responses show prevalent individual differences that include also individuals with strong object orientation responses. (**I**) The histograms for aSD indicate that *DGRP-859* flies (N = 59) show variability comparable to that of CS flies. The distribution is shifted toward higher aSDs.

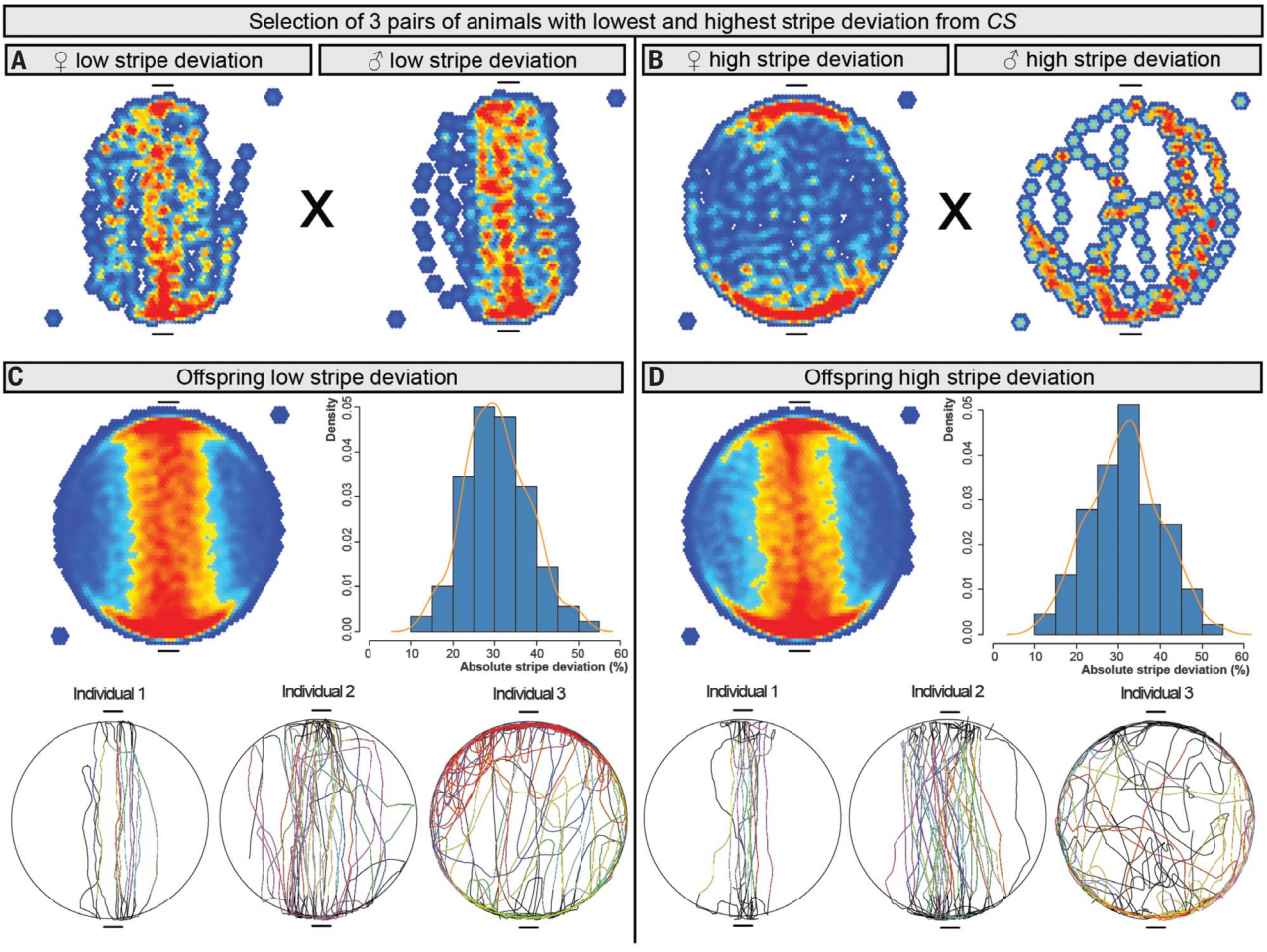

Fig. 2. Individual variation is independent of genetic selection. (**A** and **B**) The three lowest- (A) and highest-scoring couples (B) for aSD were chosen from a population of 47 *CS* males and 37 virgin *CS* females. The heatmaps in the top row show, from left to right: (i) the three virgin females and (ii) males with the lowest aSD, (iii) the three virgin females, and (iv) males with the highest aSD. (**C** and **D**) The offspring of these two populations are shown in the middle row separated by a black stripe. The behavioral heatmaps and variability histograms of the two populations of offspring are statistically indistinguishable (N = 180 for both; two-way analysis of variance (ANOVA) and Tukey HSD as post hoc test; p = 0.22). The bottom row shows examples of individuals representing the range of variability in both populations.

reduced genetic diversity affects behavioral stability. We performed repeated testing of *DGRP-639* and *DGRP-859* individual flies and found that both inbred strains showed temporally stable individual responses (Fig. 3, F and G, and fig. S5, A to C).

Together, the data show that individual variability in object orientation is a nonheritable, temporally stable trait that is independent of sex, genetic background, and genetic diversity. Where in the brain might such individuality in visual behavior originate?

A variable set of commissural visual interneurons

In 1982 Bülthoff (*30*) suggested, based on work by Zimmermann (*31*) and Götz (*32*), that object position processing in *Drosophila* (*33*) requires qualitative asymmetry of the visual percept of an object. However, direct evidence for this notion is lacking, especially that the sizes of the left and right eyes of the same fly are highly correlated (*34*). In 1986, while analyzing object responses in motion-blind flies, Heisenberg and colleagues suggested that binocular interactions, through higher-order commissural visual interneurons, are required for object orientation (*35*). Putting the two predictions together we hypothesized that variation in object orientation responses is regulated by the variation in the asymmetry of a higher-order contralateral visual circuit innervating the frontal visual field. The DCNs match this predicted circuit (Fig. 4A).

To obtain a comprehensive description of DCN wiring, we extended the previous analyses of DCNs that were based on 16 female flies (*18*), to 103 males and females. We found that the number of DCNs varied from 22 to 68 cells, with a range of 11 to 55 L-DCNs and 6 to 23 M-DCNs (Fig. 4B and fig. S8, A and B). In addition, we observed a distribution of variation in medulla-targeting asymmetry by M-DCNs (Fig. 4C, histogram distributions; fig. S8B). The distribution of all DCN asymmetries showed a peak of low asymmetries, although extreme asymmetries were present but rare. Finally, three-dimensional reconstruction showed that M-DCN axons terminate in the posterior medulla (movies S4 to S6), where visual columns from the frontal visual field are located, and the DCN wiring pattern in the medulla does not change in the adult (fig. S9 and movies S7 and S8).

Individual wiring variability drives behavioral individuality

DCNs represent an ideal candidate for an intrinsically asymmetric population of contralateral higher-order interneurons to mediate object responses (*35*). To test this hypothesis,

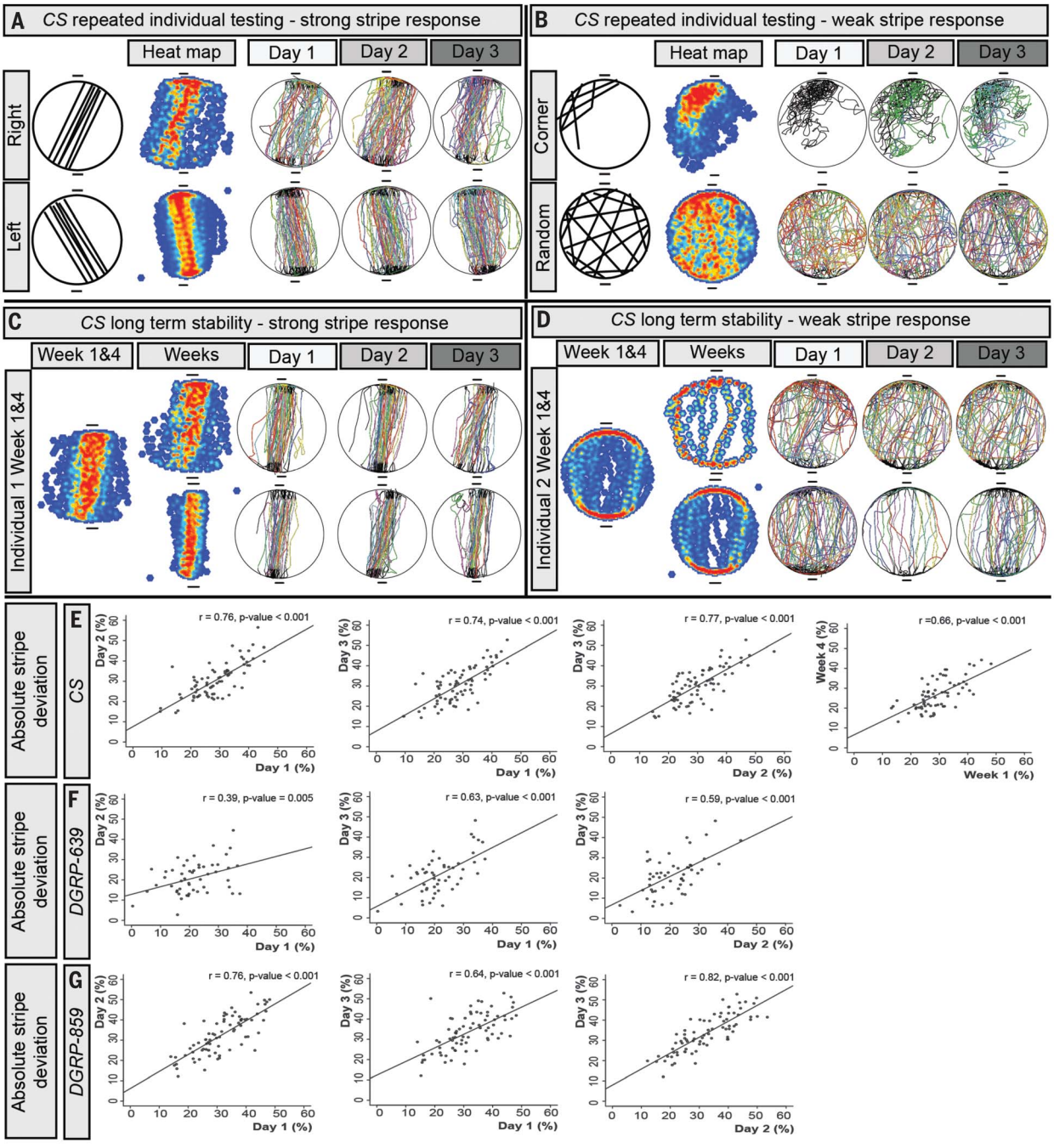

Fig. 3. Individual variation of *Drosophila* object orientation responses is stable over time. Adult *CS* flies (N = 74) were repeatedly tested over the duration of 3 days and several weeks. The flies showed marked stability in their responses irrespective of whether they responded strongly or weakly to the visual cue, or even showed no response toward the visual cue at all. (**A**) Two different examples of *CS* flies with low aSD. The heatmap and the individual tracks for the 3 days show persistent behavior. Even the angle toward the stripes is conserved throughout the 3 days. The upper row is right shifted, and the bottom row is left shifted. (**B**) Two different examples of *CS* flies with high aSD. The positional preferences are conserved between the different days. The upper row shows an animal with local preferences and the lower one performs a random walk. (**C** and **D**) Two different examples of *CS* flies with strong (individual 1) and high aSD (individual 2) that show persisting behavior throughout three consecutive days and several weeks. (**E**) Statistical analysis for aSD shows that the *CS* responses of the different days and weeks are correlated. The Pearson correlation coefficient for day 1 versus day 2 is 0.76 with $p < 0.001$. For day 1 versus day 3, the correlation coefficient is 0.76 with $p < 0.001$. For day 2 versus day 3, the correlation coefficient is 0.76 with $p < 0.001$. For week 1 versus week 4, the correlation coefficient is 0.66 with $p < 0.001$. (**F**) Similar to the *CS* data, the responses for *DGRP-639* were moderately to strongly correlated (N = 52, animals with low path length were removed; see fig. S3A for examples). The Pearson correlation coefficient for day 1 versus day 2 is 0.39 with $p = 0.0047$. For day 1 versus day 3, the correlation coefficient is 0.63 with $p < 0.001$. For day 2 versus day 3, the correlation coefficient is 0.59 with $p < 0.001$. (**G**) The correlation between days for *DGRP-859* (N = 76) even exceeds the data for *CS*. The Pearson correlation coefficient for day 1 versus day 2 is 0.76 with $p < 0.001$. For day 1 versus day 3, the correlation coefficient is 0.64 with $p < 0.001$. For day 2 versus day 3, the correlation coefficient is 0.82 with $p < 0.001$.

we first asked whether the DCNs were required for object orientation. Inactivating either all DCNs or only M-DCNs resulted in a strong increase in aSD (Fig. 4, D and E, and fig. S8, C and D). Next, we queried the relationship between individual variability in object orientation behavior and individual variability in DCN wiring (N = 103) (fig. S10). Unbiased correlation analysis between 36 behavioral parameters and 37 prominent DCN anatomical features (Fig. 5A and fig. S11, A to C) showed that left-right asymmetry in M-DCN innervation correlated with an individual's aSD (Fig. 5C, r = −0.67) and other interdependent parameters (fig. S11A). Individuals with high

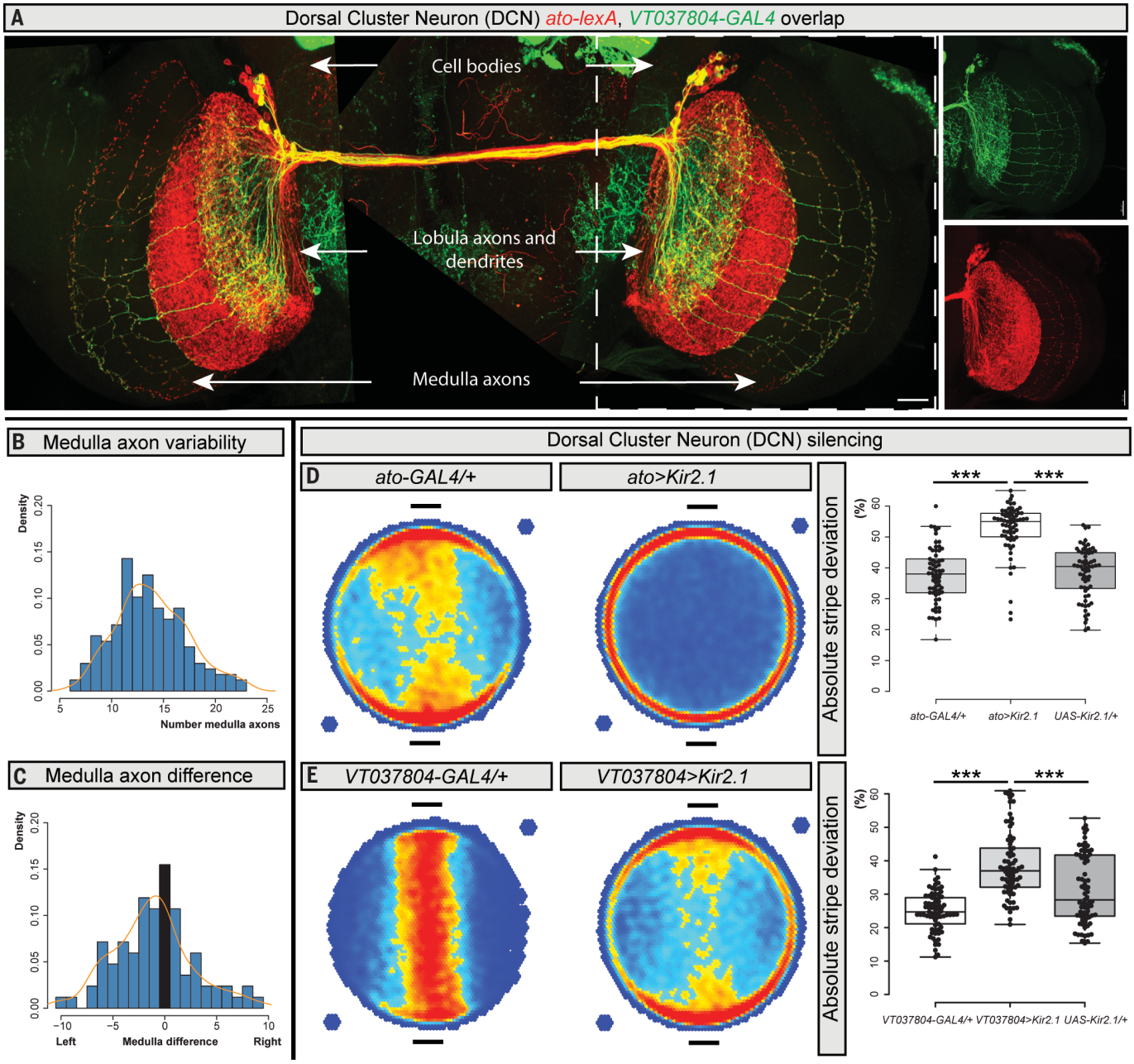

Fig. 4. Normal stripe responses require DCN function. (**A**) The DCNs are commissural neurons in the visual system of the fly. The DCNs have dorsally located cell bodies that send out an ipsilateral dendrite and a contralateral axon. This axon innervates either the visual neuropil lobula or medulla. Two independent driver lines are shown for the DCN neurons: *ato-lexA* (red, *lexAOP-myr-tdTomato*) marks all DCNs whereas *VT037804-GAL4* (green, *UAS-myr-GFP*) marks only the M-DCN neurons that innervate the medulla. (**B** and **C**) The DCNs display high variability in their axonal branching pattern, as shown for three individual brains. Statistical analysis shows that the number of medulla axon branches ranges from 6 to 23 axons with a mean of 13.99 (B). The medulla asymmetry ranges from 0 to 10 axons with a mean of 2.98 (C). (**D**) DCN neuron silencing leads to an increase in aSD. The heatmap of the control population of *ato-GAL4/+* flies shows a normal response in the two-stripe arena. This is lost upon silencing of DCN neurons in *ato>Kir2.1* animals. Statistical analysis (N = 57 to 63) of aSD shows that *ato>Kir2.1* animals show higher aSD than the controls (two-way ANOVA and Tukey HSD as post hoc test, $p < 0.001$). Higher aSD means that the animals fixate the stripes less. (**E**) Similar results are obtained by M-DCN neuron silencing with *VT037804-GAL4*. The heatmap of the control population of *VT037804-GAL4/+* flies shows normal object orientation in the two-stripe arena. This is lost upon silencing of DCN neurons in *VT037804>Kir2.1* animals. Statistical analysis (N = 72) of aSD shows that *VT037804>Kir2.1* animals show higher aSD than the controls ($p < 0.001$). Scale bars, 20 μm.

M-DCN asymmetry have a low aSD, whereas individuals with symmetric M-DCN have a high aSD (Fig. 5, B and C). To test if DCN wiring asymmetry is a functional driver of individual object orientation behavior, we silenced DCNs and repeated the analyses. This abolished the correlation between M-DCN asymmetry and aSD, but not stripe detection per se (Fig. 5, D and E, r = −0.002 and figs. S12 and S13).

DCN asymmetry determines object orientation in individuals

Our data show that nonheritable developmental variation in DCN wiring asymmetry is necessary for creating variability in object

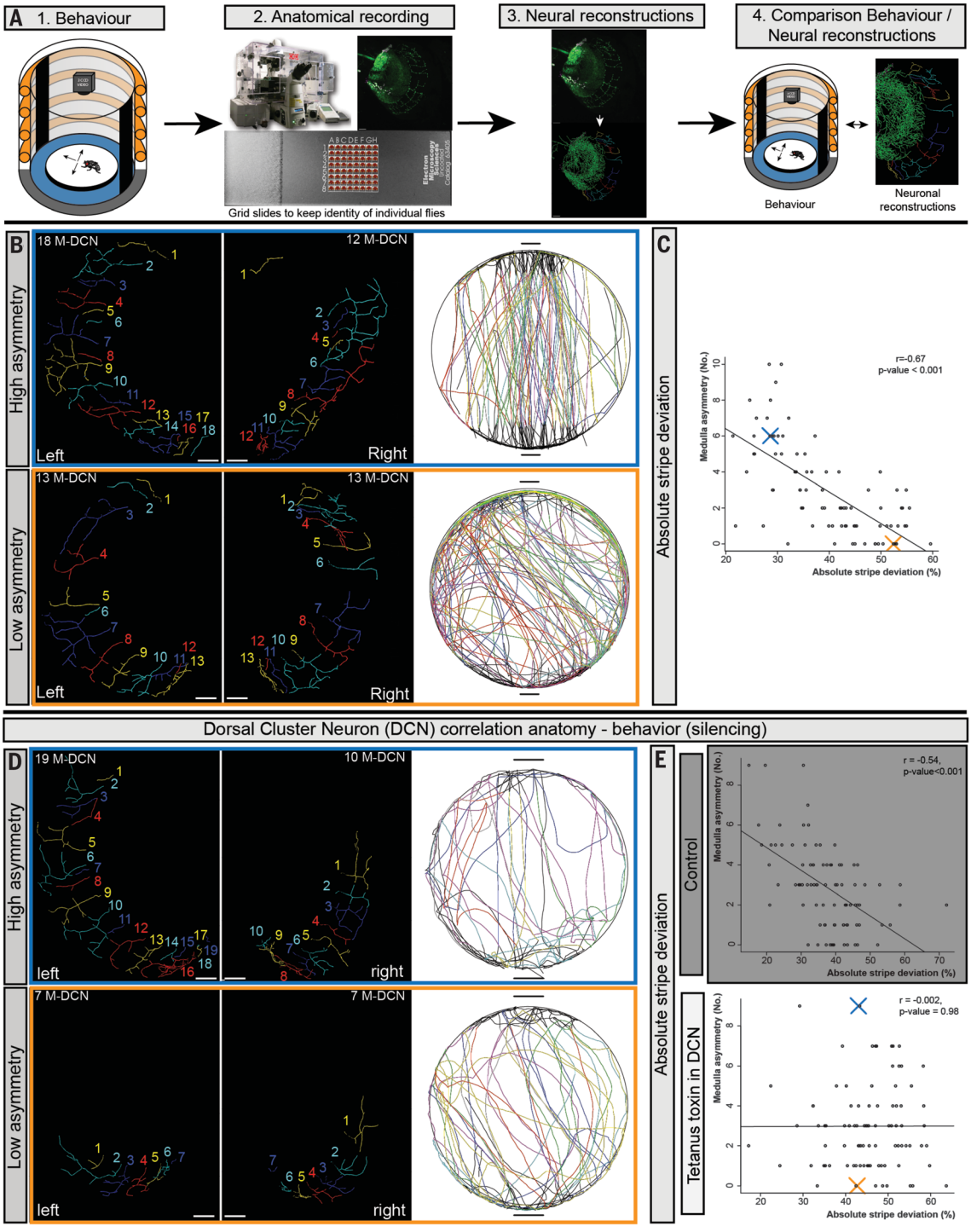

Fig. 5. Individual variation of anatomical brain asymmetry regulates behavioral variation. (**A**) To correlate behavioral variation with brain anatomical variation, flies were tested behaviorally in the Buridan arena, their brains dissected and stained, and DCN anatomy imaged, keeping individual information intact. After computational analysis of fly tracks and automated neuronal reconstruction of the brain anatomy, a cross-correlational analysis of both data sets was performed. (**B**) Animals with high left-right asymmetry of DCN axonal projections showed better performance than animals with lower asymmetry. The colored numbers show the reconstructed medulla axons in each brain hemisphere. (**C**) Statistical analysis (N = 103) shows that the medulla asymmetry correlates (r = 0.67, p < 0.001) with aSD. The blue and orange crosses mark the position of the blue and orange individuals shown in (B). (**D**) DCN silencing with tetanus toxin results in the loss of a correlation between medulla right-left asymmetry and aSD. High-asymmetry and low-asymmetry animals show approximately the same behavioral performance. (**E**) Statistical analysis shows that DCN silencing with tetanus toxin (TNT, N = 92) results in the loss of anatomy behavior correlations (r = −0.002, p = 0.98; control: N = 89, r = −0.54, p < 0.001, shaded dark gray). The examples of (D) are marked with a blue and orange cross in the correlation plot. Scale bars, 20 μm.

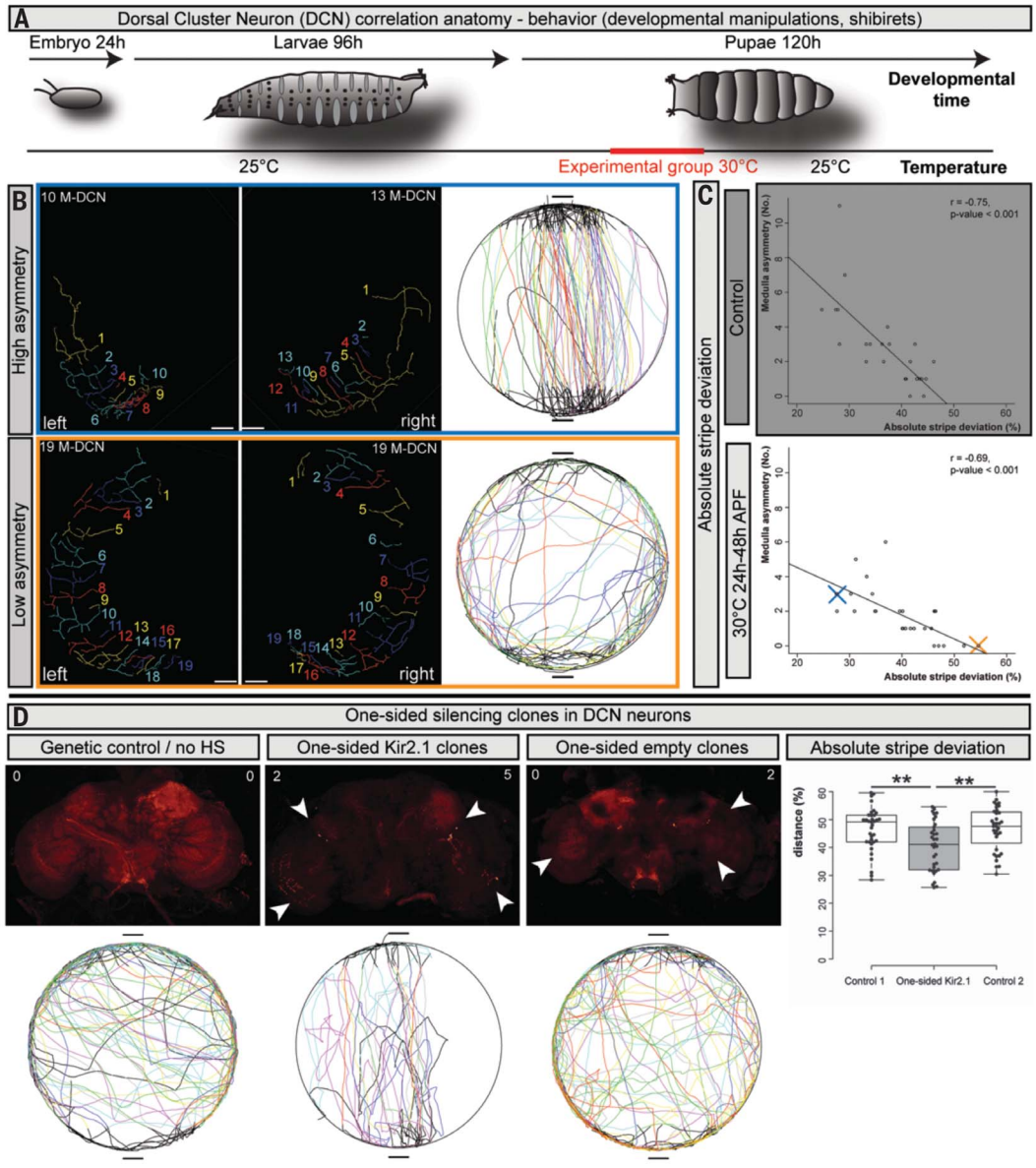

Fig. 6. Individual variation of anatomical brain asymmetry suffices for behavioral variation. (**A**) Schematic for the developmental inhibition of endocytosis using *UAS-shibire^{ts}* during the critical period (24 to 48 hours after puparium formation). The manipulation to change asymmetry is performed at the time of the choice between M-DCN or L-DCN (*18*). (**B**) Blocking endocytosis during DCN development increased the proportion of individuals with symmetric wiring and correspondingly aSD, with no effect on the correlation between anatomy and behavior in single flies. (**C**) Correlation curve of the *UAS-shibire^{ts}* individuals described in (B) (N = 27, r = −0.69, p < 0.001; control: N = 25, r = −0.75, p < 0.001, shaded dark gray). (**D**) Directed induction of one-sided clones in M-DCNs expressing Kir2.1 results in stronger object orientation responses than in the genetic control [same genotype, no heat shock (HS) clonal induction, p = 0.007] and in the HS control (identical genotype but lacking *UAS-Kir.2.1*, p = 0.006). Data were analyzed by two-way ANOVA and Tukey test. Scale bars, 20 μm.

orientation behavior across individuals. We therefore wondered if the changed object orientation responses in the DGRP strains reflect DCN asymmetry alterations. We found that the low aSD strain *DGRP-639* displayed more DCN wiring asymmetry, and the high aSD strain *DGRP-859* less DCN wiring asymmetry (fig. S14), consistent with our hypothesis. Next, we developmentally rewired the DCNs either by blocking endocytosis to inhibit developmental signaling among DCNs or by activating the Notch pathway, both in a DCN-specific fashion. This resulted in reduced DCN wiring asymmetry and a correspondingly higher aSD, while preserving the correlation between wiring and behavior (Fig. 6, A to C, and figs. S15 and S16). Finally, we genetically engineered flies to generate one-sided DCN clones expressing the neuronal silencer Kir2.1. Animals with asymmetrically silenced clones showed lower aSD scores than controls with unsilenced clones or no clones at all (Fig. 6D and fig. S17). Together, these data causally link DCN wiring asymmetry to object orientation responses.

Finally, to test our hypothesis further, we asked if generating any asymmetry in visual processing is sufficient to override high stripe deviation. Among 79 *CS* flies tested, we selected the 20 with the highest aSD indices (>40), performed monocular deprivation, and tested them again. This resulted in a reduction of aSD in these flies, as well as in the entire population (fig. S18).

Discussion

The origins of behavioral individuality are a central question in neuroscience, psychology, and evolution. The discovery of stable individual traits in nonhuman vertebrates (*16*) and invertebrates facilitated research on behavioral variation (*10*, *14*) and offered both genetic (*11*, *12*, *36*) and neuromodulatory (*11*, *15*, *36*) explanations for behavioral idiosyncrasies. Here we establish a link between variability in the development of the brain and the emergence of individuality of animal behavior. Our work shows that intrinsically stochastic mechanisms of brain wiring give rise to intraindividual variation of left-right asymmetry in the innervation of the fly visual areas, which explains the individuality of behavioral differences in object responses. The amenability of the relatively complex *Drosophila* brain to multiscale analysis, from the molecular to the behavioral, at single-animal resolution makes it a model for understanding the emergence of individuality at each of these scales. We speculate that

similar mechanisms and consequences will hold true in other species, including humans.

Previous work in *Drosophila* visual behavioral neuroscience led to the proposal that asymmetry in visual information processing influences object responses. Where such functional asymmetry lay and how it might arise has, until now, remained unclear. Independently, the study of object responses in motion-blind mutants led Heisenberg and colleagues to propose a hypothetical contralateral circuit dedicated to object responses in the frontal visual field (*28*, *30*–*32*, *35*). Our discovery that DCN asymmetry drives object orientation responses in individuals is an elegant solution combining both predictions: a contralateral asymmetric visual circuit that regulates object orientation in the frontal visual field. Future work will reveal the exact physiological consequences of morphological asymmetry, such as whether wiring asymmetry induces timing differences as in auditory navigation (*37*) or whether the absolute differences are simply summed up.

Our work provides evidence for the generation of multiple brain and behavior phenotypes from the same genotype via developmental stochasticity and noise. This can serve as a robustness factor for both the individual and the population by increasing the chances of survival of any given genome in case of strong selection pressure (*22*).

REFERENCES AND NOTES

1. P. M. Visscher, *Nat. Genet.* **40**, 489–490 (2008).
2. G. Vogt *et al.*, *J. Exp. Biol.* **211**, 510–523 (2008).
3. H. Pakkenberg, J. Voigt, *Acta Anat. (Basel)* **56**, 297–307 (1964).
4. J. S. Allen, H. Damasio, T. J. Grabowski, *Am. J. Phys. Anthropol.* **118**, 341–358 (2002).
5. A. Mohr, M. Weisbrod, P. Schellinger, M. Knauth, *Brain Res. Cogn. Brain Res.* **20**, 106–110 (2004).
6. Y. H. Chou *et al.*, *Nat. Neurosci.* **13**, 439–449 (2010).
7. V. Budnik, Y. Zhong, C. F. Wu, *J. Neurosci.* **10**, 3754–3768 (1990).
8. E. R. Graf, R. W. Daniels, R. W. Burgess, T. L. Schwarz, A. DiAntonio, *Neuron* **64**, 663–677 (2009).
9. C. S. Goodman, *J. Comp. Neurol.* **182**, 681–705 (1978).
10. W. Schuett *et al.*, *Dev. Psychobiol.* **53**, 631–640 (2011).
11. J. S. Kain, C. Stokes, B. L. de Bivort, *Proc. Natl. Acad. Sci. U.S.A.* **109**, 19834–19839 (2012).
12. J. F. Ayroles *et al.*, *Proc. Natl. Acad. Sci. U.S.A.* **112**, 6706–6711 (2015).
13. A. Renart, C. K. Machens, *Curr. Opin. Neurobiol.* **25**, 211–220 (2014).
14. S. D. Gosling, *Soc. Personal. Psychol. Compass* **2**, 985–1001 (2008).
15. S. Stern, C. Kirst, C. I. Bargmann, *Cell* **171**, 1649–1662.e10 (2017).
16. C. Pantoja *et al.*, *Neuron* **91**, 587–601 (2016).
17. E. Marder, *Neuron* **76**, 1–11 (2012).
18. M. Langen *et al.*, *eLife* **2**, e00337 (2013).
19. M. Zschätzsch *et al.*, *eLife* **3**, e01699 (2014).
20. P. R. Hiesinger, B. A. Hassan, *Trends Neurosci.* **41**, 577–586 (2018).
21. K. Honegger, B. de Bivort, *Curr. Biol.* **28**, R8–R12 (2018).
22. D. N. Fisher, M. Brachmann, J. B. Burant, *Anim. Behav.* **138**, e1–e6 (2018).
23. T. J. H. White, *J. Am. Acad. Child Adolesc. Psychiatry* **58**, 1042–1050 (2019).
24. B. A. Hassan *et al.*, *Neuron* **25**, 549–561 (2000).
25. H. Otsuna, K. Ito, *J. Comp. Neurol.* **497**, 928–958 (2006).
26. X. Zheng *et al.*, *EMBO J.* **25**, 615–627 (2006).
27. J. Colomb, L. Reiter, J. Blaszkiewicz, J. Wessnitzer, B. Brembs, *PLOS ONE* **7**, e42247 (2012).
28. H. Bülthoff, K. G. Götz, M. Herre, *J. Comp. Physiol.* **148**, 471–481 (1982).
29. T. F. Mackay *et al.*, *Nature* **482**, 173–178 (2012).
30. H. Bülthoff, *Biol. Cybern.* **45**, 71–77 (1982).
31. G. Zimmermann, thesis, Eberhard-Karls-Universitaet Tübingen, Tübingen, Germany (1975).
32. K. G. Götz, *Naturwissenschaften* **62**, 468–475 (1975).
33. W. Reichardt, *Naturwissenschaften* **60**, 122–138 (1973).
34. J. Vollmer *et al.*, *Development* **143**, 1482–1490 (2016).
35. B. Bausenwein, R. Wolf, M. Heisenberg, *J. Neurogenet.* **3**, 87–109 (1986).
36. S. M. Buchanan, J. S. Kain, B. L. de Bivort, *Proc. Natl. Acad. Sci. U.S.A.* **112**, 6700–6705 (2015).
37. T. P. Franken, M. T. Roberts, L. Wei, N. L. Golding, P. X. Joris, *Nat. Neurosci.* **18**, 444–452 (2015).

ACKNOWLEDGMENTS

We thank the Bloomington stock center (NIH P40OD018537) and Gilad Barnea for providing flies used in this study. We thank L. Fenk for insightful discussions during the initiation phase of the project and B. van Swinderen and all members of the Hassan, Hiesinger, and Wernet lab for support and valuable comments. We also thank the VIB Bio Imaging Core. **Funding:** This work was supported by the ICM Big Brain Theory Program, the program "Investissements d'avenir" (ANR-10-IAIHU-06), an ANR grant (ANR-19-CE16-0009-01), The Einstein-BIH program, the Paul G. Allen Frontiers Group, VIB, the WiBrain Interuniversity Attraction Pole network (Belspo), the FLiACT Marie-Curie Initial Training Network (FP7/2007-2013) (to B.A.H.), NIH (RO1EY018884) and the German Research Foundation (DFG: SFB 958, SFB186) (to P.R.H.), FU Berlin (to P.R.H. and M.W.), as well as EMBO Long Term Postdoctoral Fellowships (to G.A.L. and R.K.E.), VIB Omics postdoctoral fellowship (to R.K.E.), and the Marie Skłodowska Curie Actions postdoctoral fellowship in FP7 and Horizon 2020. Further support for G.A.L. was provided by FU Berlin (to P.R.H.). B.A.H. is an Allen Distinguished Investigator and a BIH-Einstein Visiting Fellow. **Author contributions:** G.A.L. and B.A.H. conceived the study, designed the experiments, and wrote the manuscript. G.A.L. conducted all behavioral experiments, immunohistochemistry, and all data analysis. M.A., S.B.D., and L.H. helped with the neuronal reconstructions. M.B. helped with control behavioral experiments. G.L. and R.K.E. provided technical expertise, G.L. helped with building the Buridan arena, and R.K.E. wrote the Python analysis software. A.D.S. shared unpublished data and reagents and provided technical expertise for behavioral experiments. M.W. and P.R.H. provided expertise and equipment and helped write the manuscript. **Competing interests:** The authors declare no competing interests. **Data and materials availability:** All data are available in the manuscript or the supplementary materials.

SUPPLEMENTARY MATERIALS

science.sciencemag.org/content/367/6482/1112/suppl/DC1
Materials and Methods
Figs. S1 to S18
Movies S1 to S8
References (*38*–*54*)

View/request a protocol for this paper from *Bio-protocol*.

18 January 2019; resubmitted 26 September 2019
Accepted 27 January 2020
10.1126/science.aaw7182

A neurodevelopmental origin of behavioral individuality in the *Drosophila* visual system

Gerit Arne Linneweber, Maheva Andriatsilavo, Suchetana Bias Dutta, Mercedes Bengochea, Liz Hellbruegge, Guangda Liu, Radoslaw K. Ejsmont, Andrew D. Straw, Mathias Wernet, Peter Robin Hiesinger and Bassem A. Hassan

Science **367** (6482), 1112-1119.
DOI: 10.1126/science.aaw7182

Diversity from development

When given a line to follow, some fruit flies do so carefully and others weave. Linneweber *et al.* now show that these behaviors are stable for an individual but diverse in an isogenic population. Key to generating individual diversity in the population is the inherent chaos of normal development. A set of neurons in the visual system is wired up in a variable manner, resulting in brain circuit asymmetry unique to each fly that guides its line-walking behavior. With more asymmetry in its brain circuit, a fly is better able to orient to the line.

Science, this issue p. 1112